

Cu-bearing signatures from multi-element geochemical data, a correct strategy to implement a convolutional autoencoder algorithm

Mobin Saremi ^a, Seyyed Ataollah Agha Seyyed Mirzabozorg ^b, Abbas Maghsoudi ^a, Maysam Abedi ^{b,*} and Ramin DehghanNiri ^b

^a Department of Mining Engineering, Amirkabir University of Technology, Tehran, Iran.

^b School of Mining Engineering, College of Engineering, University of Tehran, Tehran, Iran.

Article History:

Received: 17 August 2024.

Revised: 01 October 2024.

Accepted: 29 October 2024.

ABSTRACT

Recent advancements in autoencoders and their variants have notably enhanced the detection of multi-element geochemical signatures linked to ore occurrences. This research employed a convolutional autoencoder algorithm (CAE) to identify geochemical anomalies, leveraging the algorithm's ability into account the spatial correlation within the geochemical dataset. In this framework, two stream sediment datasets were generated in the Feizabad district using a conceptual modelling approach alongside a big data analysis strategy. These datasets were individually fed into the CAE model to identify multi-element geochemical anomalies based on the reconstruction error in an unsupervised manner. A comparative analysis of two geochemical prospectivity models and the simplified geological map of Feizabad demonstrates a strong spatial correlation between the identified anomaly regions and known mineral occurrences, which are distributed across andesite, tuff, and Eocene-Oligocene intrusive rocks. However, a quantitative assessment using prediction-area plots indicates that the multi-element geochemical map derived from the conceptual model exhibits a higher prediction rate (72%) compared to the geochemical prospectivity map generated through the big data approach (63%).

Keywords: Stream sediment geochemistry, Deep learning, Big data analytics, Unsupervised anomaly detection, Feizabad district.

1. Introduction

Recognizing geochemical anomalies through stream sediment samples is a fundamental task in regional-scale geochemical exploration [1-4], as it helps exploration geologists accurately delineate exploration targets and improve their understanding of the mineralization sought. Stream sediment samples are among the best exploration data and provide important information about the migration of elements from alteration and mineralization zones [1]. These samples are the product of erosion and weathering of the upper rocks in the catchment basin [5]. The main goal of stream sediment geochemistry is to separate high-potential zones from unfavorable regions, resulting in a smaller search space for subsequent mineral exploration programs and cost reduction [6, 7]. The spatial distribution of ore elements in these sediments is significantly influenced by various complex events, including fluid movements, structural factors and hydrothermal processes [8]. As a result, stream sediment geochemical data exhibit complex nonlinear systems. This complexity and nonlinear relationship may indicate hidden patterns and anomalies associated with ore mineralization.

Over the past decades, various methods have been developed to detect geochemical anomalies and identify patterns associated with mineralization in geochemical datasets [9, 10]. In general, these methods can be divided into main groups, such as frequency-based and frequency-spatial-based statistical approaches [11-14]. Some classical statistical methods include mean \pm k standard deviation [15], exploratory data analysis [16], and multivariate analysis (e.g., PCA-FA) [6, 17-19]. These methods are based on the frequency distribution and

ignore the spatial structures/correlation of the stream sediment geochemical data [20]. To address this issue, advanced spatial statistical methods, such as spatially weighted factor analysis [21], the fractal/multifractal approach [22-25], and multivariate geostatistics tools [26] have been successfully proposed in the context of geochemical data analysis. However, these techniques depend on several specific assumptions, such as normal distribution and linear relationship [27]. In addition, due to the complexity of geological phenomena and the multi-step nature of mineral systems, geochemical data exhibit high dimensionality, spatial correlation, and nonlinear complexity [6, 11, 27, 28]. For these reasons, the statistical distribution of these data is sophisticated [29]. Hence, the mentioned techniques utilized in the analysis of stream sediment geochemical data have limitations and cannot completely model nonlinear relationships between the elements associated with mineral deposits.

Recently, various machine learning (ML) and deep learning (DL) algorithms have been successfully applied for geochemical anomaly detection and lithological classification [11, 30-33]. These algorithms can be divided into two main categories, namely supervised and unsupervised methods. Supervised algorithms (e.g., CNN [34, 35] and ANN [36]) could integrate multivariate geochemical data to extract complex and hidden mineralization-related information without any assumptions about data distribution [37]. However, the main challenge in the implementation and training of supervised algorithms is that a large number of labeled samples are required [37]. Additionally, the lack

* Corresponding author. E-mail address: maysamabedi@ut.ac.ir (M. Abedi).

of access to negative ground truth samples in the regional studies leads to a further limitation in utilizing these algorithms [38]. In contrast to supervised algorithms, unsupervised algorithms do not encounter the aforementioned challenges, as they do not rely on labeled data for training [38]. Several studies have adopted unsupervised learning algorithms, such as one-class support vector machine [39], isolation forest [40, 41], clustering [42-44], CRBM [45, 46], deep AutoEncoder (AE), and its variants [38, 47-49] for geochemical anomaly recognition and mineral prospectivity mapping (MPM). In recent years, the deep AE and its variants have attracted more interest than other algorithms in the context of geochemical anomaly detection. They are characterized by their significant ability to learn intricate nonlinear patterns and detect nonlinear anomalies in input data [27].

In the training phase, the AE is fed with all geochemical datasets, consisting mainly of non-anomalous samples. Through training, the model only learns to reconstruct the background samples well, and anomalous samples contribute limitedly to the learning process due to their non-representative features, resulting in weaker reconstruction and higher reconstruction error compared to normal samples [38, 50]. Xiong and Zuo (2016) explored the application of deep AE in recognizing multivariate geochemical anomalies associated with iron mineralization [47]. They normalized the concentration values for five elements related to skarn-type Fe mineralization, namely Cu, Pb, Mn, Zn, and Fe_2O_3 , and used them to train the deep AE. Their results demonstrate the usefulness of the deep AE network in recognizing multivariate geochemical anomalies for mineral exploration. However, the basic AE is classified as a spectral-based method, where each sample (cell) is fed into the model as a feature vector [51]. Hence, the model ignores the spatial correlation among neighboring samples and focuses only on mineralization-related features within each sample. To address this challenge, some studies proposed the Convolutional AutoEncoder (CAE), which improves the basic architecture of simple AEs by replacing fully connected layers with convolutional and pooling layers [37, 48, 52]. A CAE effectively reconstructed geochemical samples by considering their spatial patterns and local spatial structures, thereby facilitating the recognition of multivariate geochemical anomalies caused by reconstruction errors [48]. Various studies confirm the strong performance of CAE in recognizing multivariate geochemical anomalies related to mineralization [37, 48, 52]. Xiong and Zuo (2021) successfully employed a convolutional denoising autoencoder (CDAE) to detect multivariate geochemical anomalies associated with mineralization from geochemical data covering 39 major and trace geochemical elements [48].

The aim of this paper is to recognize the multi-element geochemical footprints/signatures associated with hydrothermal copper mineralization in the Feizabad region by applying the CAE algorithm. To successfully execute a robust CAE algorithm, it is important to develop a suitable strategy that is customized according to the input feature vector. Therefore, two stream sediment geochemical datasets were generated based on the conceptual model (partial data) and big data analytic approach (full data). In the next step, the data-driven prediction-area plot was utilized for the quantitative assessment of the geochemical prospectivity models. Finally, an effective geochemical prospectivity model associated with hydrothermal copper mineralization was identified. Finally, an effective geochemical prospectivity model associated with hydrothermal copper mineralization was identified, introducing favorable areas for subsequent mineral exploration programs.

2. Geological setting of the Feizabad district

The Feizabad district lies within the Moaleman-Torbat-e-Heydaryeh metallogenic belt in Khorasan Razavi Province, northeastern Iran [53]. This geological region is a significant area for the exploration of various mineral deposits. The mentioned metallogenic belt is bounded in the southwest by the Dorouneh fault. The Dorouneh strike-slip fault is the main fault in the Feizabad district which divides the area into two northern and southern sections [54]. The northern section of the

1:100,000 geological sheet of Feizabad consists of sedimentary units, different types of tuffs, Tertiary volcanic and pyroclastic rocks, and Eocene-Oligocene intrusive rocks [54]. From a geological point of view, this part is therefore more important than the southern section. The tectonic features and geological setting of the northern section make it a prospective area for the exploration of various types of mineralization, such as hydrothermal copper. There are 13 hydrothermal Cu deposits and occurrences in the Feizabad area, most of which are located near volcanic and Eocene-Oligocene intrusive rocks. These deposits include IOCG, epithermal base and precious metals, Cu-Au porphyry, and vein-type Cu [2]. Figure 1 shows a simplified geological map of Feizabad with a 1:100,000 scale. In this region, copper, iron, and gold mineralization have been observed in proximity to intrusive rocks. Additionally, alteration zones have resulted from the intrusion of granodiorite and granite units. Faults and fractures have controlled the fluid flows, and have played a major role in their formation. From an exploration geochemistry perspective, previous studies have shown that the association of elements, such as Zn, Pb, As, Sb, Mo, and Sn may be related to vein-type mineralization of these elements within the volcanic units of the area. Moreover, the association of Cu, Hg, and Au elements may explain the presence of porphyry deposits and possibly IOCG in the intrusive rocks and adjacent volcanic units [2].

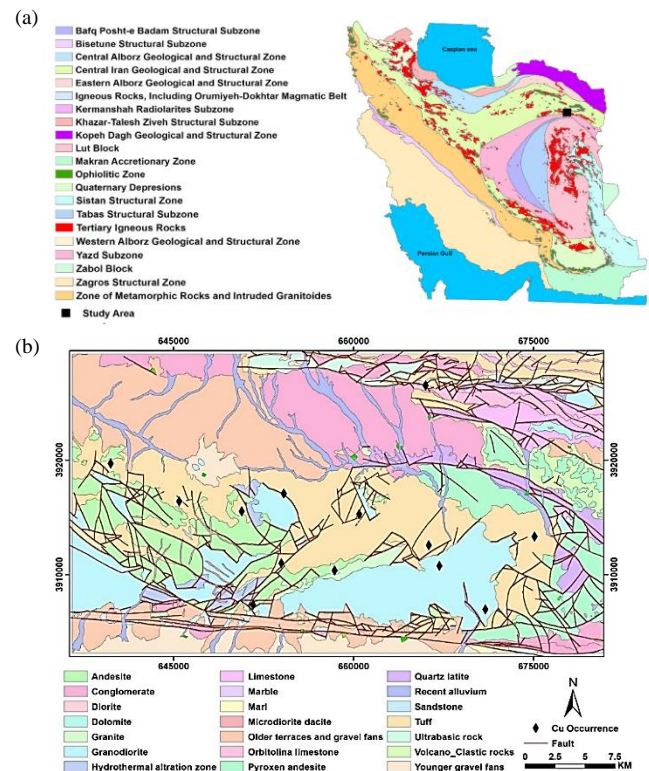


Figure 1. The location of the Feizabad district on the map of structural zones of Iran (a) and the simplified geological map of the Feizabad district (b).

The Kuh-e-Zar deposit is a type of IOCG mineralization in the Feizabad district, in which the quartz–specular hematite–gold vein is considered the first and most important mineralized vein [55]. The Namegh Cu-Au prospect is located in the northern region of the Feizabad district [56]. Based on the Feizabad geological map, the lithology of the Namegh area includes white brecciated tuff, ignimbrite, lapilli tuff, and green sandy tuff, all of Eocene age. Previous research has demonstrated that, alongside these rocks, there are numerous intrusive rocks, such as diorite, monzodiorite, and monzonite, which manifest as stocks and dikes [56]. This has resulted in significant mineralization and extensive hydrothermal alteration in the region. Mineralization is observed in monzodioritic intrusions and volcanic rocks, and significant

Cu and Au anomalies are identified primarily within these geologic units. It can be concluded that monzodioritic dikes and stocks are the main sources of mineralization in the Namegh region [56]. The Tanorcheh is another deposit in the Feizabad region that has been recognized as a valuable anomaly zone through stream sediment geochemical studies. Generally, the geological characteristics, alteration features, and geochemical analyzes indicate that the Feizabad region has significant potential for the presence of hydrothermal copper deposits, such as porphyry deposits. Cu, Fe, and Au mineralization has been commonly observed in proximity to the intrusive rocks and faults in this region.

3. Geospatial data set

The Geological Survey and Mineral Exploration of Iran (GSI) conducted a systematic collection of 1,033 stream sediment samples from the Feizabad region at a scale of 1:100,000. After initial preparation and coding, these samples were analyzed for 28 elements and Au, respectively, using ICP-OES and Fire-Assay methods. According to the quality of the geochemical data, a dataset consisting of 26 major and trace geochemical elements related to the 587 stream sediment samples collected in the north of the Feizabad district was used. Basic statistical descriptions (such as mean, standard deviation, minimum, maximum, skewness, and kurtosis) for 26 element concentrations are calculated and presented in Table 1. Additionally, the study incorporated a geological map at a 1:100,000 scale for quality assessment and the locations of 13 known hydrothermal copper deposits to quantitatively evaluate the geochemical models developed through CAE.

Table 1. The basic statistical descriptions related to 587 stream sediment samples in the Feizabad district.

Elements	Minimum	Maximum	Mean	Std. deviation	Skew	Kurt
Zn	40.2	312.0	89.82	38.65	1.59	3.25
Pb	3.6	256.6	30.06	23.59	3.32	19.61
Ag	0.0	0.7	0.08	0.04	8.01	102.39
Cr	71.2	5448.2	477.39	608.06	2.80	11.25
Ni	26.3	829.6	110.60	101.60	2.74	9.96
Bi	0.1	5.0	0.33	0.39	5.86	49.83
Cu	21.3	153.9	39.48	15.57	2.77	11.46
As ₂	2.5	52.6	9.79	4.48	3.61	23.27
Sb	0.1	4.2	0.73	0.44	2.08	9.24
Co	11.6	59.0	19.89	6.04	1.96	5.78
Sn	1.0	4.2	1.83	0.46	1.02	3.81
Ba	89.4	1237.0	385.71	135.82	1.09	3.59
V	82.4	1078.0	137.22	76.73	6.76	61.96
Sr	89.2	529.8	244.62	61.09	1.00	2.21
Hg	0.0	0.1	0.01	0.01	2.04	9.81
W	0.2	8.8	1.25	0.68	2.89	25.44
B	11.0	135.7	42.45	18.89	1.78	4.75
Be	0.8	3.9	1.78	0.30	0.75	7.00
Mo	0.2	3.8	1.03	0.58	1.12	2.18
Li	11.9	71.8	29.63	6.32	1.15	4.75
Au	0.3	32.0	1.85	2.61	6.13	49.56
Rb	8.0	154.3	67.65	22.81	-0.08	-0.01
Cs	2.8	17.5	6.55	2.23	1.69	4.41
Nb	3.2	19.0	12.10	2.91	-0.24	-0.72
Th	2.1	13.7	8.73	2.53	-0.77	-0.15
U	0.6	3.0	1.76	0.41	-0.19	0.21

3.1. Geochemical data analysis

Before using DL algorithms to identify geochemical anomalies, several preprocessing steps were employed. Implementing these steps leads to the creation of high-quality geochemical datasets and improves

the performance of DL algorithms. Hence, three basic steps, including statistical preprocessing, data interpolation, and logistic function adoption were followed. In the first step, some statistical data preprocessing was applied, such as the replacement of censored values. The next step involved adopting the IDW technique to interpolate stream sediment geochemical data. Finally, the logistic function proposed by Yousefi et al. (2016) [57] was utilized to transform the data values into the fuzzy space, which is expressed as the following function:

$$F_E = \frac{1}{1+e^{-s(E-i)}} \quad (1)$$

where F_E is the value of the fuzzy membership and the assigned fuzzy score, s is the slope of the logistic function, i is the inflection point of the logistic function, and E is a weighted fuzzy evidential layer that is transformed into an interval of [0,1]. Also, the values of i and s were obtained from Eqs. 2 and 3:

$$i = \frac{E_{max}+E_{min}}{2} \quad (2)$$

$$s = \frac{9.2}{E_{max}-E_{min}} \quad (3)$$

4. Methodology

4.1. Convolutional autoencoder

Convolutional autoencoder (CAE) is an extension of a simple AE that uses convolutional layers instead of the fully connected layers, improving its ability to capture spatial features and patterns in data [58]. The schematic architecture of the CAE is illustrated in Fig. 2. Like the classic AEs, CAE consists of two main parts, namely the encoder and the decoder.

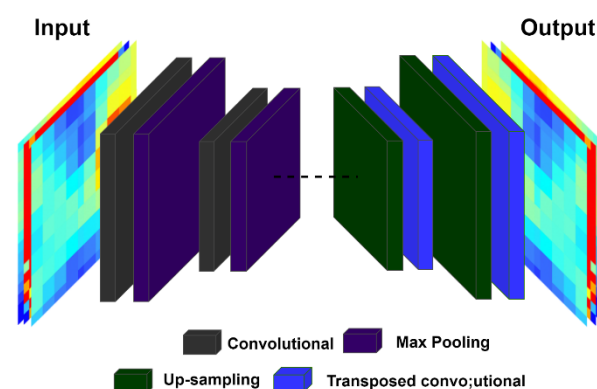


Figure 2. The schematic architecture of the simple CAE.

The encoder part employs convolution layers to extract important features and compress the input data into a lower-dimensional representation (i.e., latent space). The decoder phase then uses this compressed representation and transposed convolution layers to reconstruct the original input [59]. In addition, max-pooling and up-sampling layers are usually used in the encoder and decoder phases, respectively. Max-pooling layers downsample and shrink the feature maps created by convolution layers, while up-sampling layers increase the size of feature maps by reversing the function of max-pooling (Fig. 3).

A convolution layer is a key component of CAEs, consisting of multiple kernels (filters) that allow the network to learn and recognize spatial patterns. These kernels convolved the input data to capture important features and create feature maps (Fig. 3a). A pooling layer is typically deployed after a convolutional layer to downsample the feature maps by retaining only the most significant information (Fig. 3c). Similar to the convolution layer, the transposed convolution layer consists of a series of kernels. It increases the spatial dimensions of the

feature maps by reversing the convolution operation (Fig. 3b). The up-sampling layer increases the dimensions of feature maps (Fig. 3d). In the encoder phase, the locations of the maxima within each pooling region were recorded and then exploited using the up-sampling layer to place the values at appropriate locations [60]. This function is demonstrated as a switch variable in Fig. 3c, d.

Through the learning process, by minimizing the reconstruction error, CAE effectively learns to capture the common underlying features of the data and then reconstructs the image. This algorithm can be used for both feature extraction and unsupervised anomaly detection tasks. The former exploits the compressed representations of input data (latent space), while the latter uses the reconstruction error of samples. For unsupervised anomaly detection task, the CAE was trained on a dataset containing both normal (background) and anomalous samples. It should be noted that the dataset must mostly contain normal samples. During the training phase, the model was trained to minimize the overall reconstruction error. The CAE can then learn only the most representative and frequent patterns. As a result, anomalies contribute less to the learning process, leading to weak reconstruction compared to normally represented samples. Accordingly, the reconstruction error could be used as a measure for identifying anomalous samples with higher reconstructed error [38]. In multivariate geochemical data, this technique can be effectively used to detect anomalies, which often occupy much less area than normal samples (1.5%–5% of the total area), while the majority of the data represents the background of the study area [37].

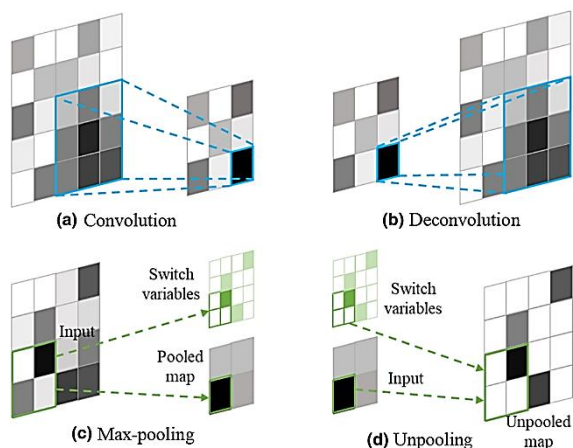


Figure 3. Demonstration of how (a) convolution, (b) deconvolution, (c) pooling and (d) up-sampling (unpooling) layer operations in the CAE [48].

4.2. CAE architecture and training phase

The architecture of the CAE used in this research includes an encoder and a decoder network (Table 2). The encoder phase begins with an input layer of size $8 \times 8 \times 26$ for the big dataset (full data) and $8 \times 8 \times 9$ for the conceptual-based dataset (partial data). The input is passed through a Conv2D layer with 128 filters using 3×3 kernels at stride 1, with a total of 30080 parameters. The extracted feature maps are then passed through a 2×2 max-pooling layer with stride 1, reducing the spatial dimensions to $4 \times 4 \times 128$. The subsequent Conv2D layer with 256 filters and 3×3 kernels at stride 1, further processes the output of the last layer, producing an output of $4 \times 4 \times 256$ with 295168 parameters. In the decoder phase, the first layer is a Conv2DTranspose layer with 256 filters and a 3×3 kernel size at stride 1, resulting in an output of $4 \times 4 \times 256$ and 590080 parameters. This is followed by an up-sampling layer that scales the output back to $8 \times 8 \times 256$. Finally, a Conv2DTranspose layer with 128 filters reduces the output to $8 \times 8 \times 128$, adding 295040 parameters to the network, before the output layer reconstructs the final image to its original size of $8 \times 8 \times 26$ for the big dataset and $8 \times 8 \times 9$ for the conceptual-

based dataset with an additional 29978 parameters. Training was conducted with an Adam optimizer, using a learning rate of 0.001, a batch size of 64, and 500 epochs. The model's performance was optimized by minimizing the mean squared error (MSE) loss function. A LeakyReLU activation function and a sigmoid activation were used for all convolutional and output layers, respectively.

To analyze the study area, a standard grid cell measuring 800×800 meters was placed over it, dividing it into patch samples of the same size. A total of 1760 cells were created and utilized for training the CAE model. The reconstruction error of each cell was calculated after the training process and used as the anomaly score. Figure 4 illustrates the methodology employed in this study to create geochemical maps associated with mineralization.

Table 2. Architecture of adopted CAE in this study for geochemical anomaly detection.

Sub-network	Layer	Output size	Param
Encoder	Input	$8 \times 8 \times 26$ and $8 \times 8 \times 9$	0
	Conv2D	$8 \times 8 \times 128$	30080
	Max-pooling	$4 \times 4 \times 128$	0
	Conv2D	$4 \times 4 \times 256$	295168
Decoder	Conv2DTranspose	$4 \times 4 \times 256$	590080
	Up-sampling	$8 \times 8 \times 256$	0
	Conv2DTranspose	$8 \times 8 \times 128$	295040
	Output	$8 \times 8 \times 26$ and $8 \times 8 \times 9$	29978

5. Geochemical dataset layout

5.1. Partial dataset

There exists a significant correlation among geochemical elements across various types of ore mineralization [18, 61]. Recognizing these meaningful relationships can provide exploration geologists with critical insights into the mineral deposits presented in an area. Furthermore, leveraging these insights enhances the likelihood of successfully identifying exploration targets. Therefore, the identification of multi-element geochemical signatures and the precise delineation of anomaly zones are essential components of regional-scale geochemical exploration [62, 63]. In this regard, various frameworks can be employed, including the application of a conceptual model of mineral deposit type being sought. This framework aligns with traditional methods, such as principal component analysis (PCA) [64, 65], factor analysis (FA) [66], and staged factor analysis (SFA) [6, 18, 67, 68] to detect geochemical footprints associated with multiple elements. Statistical techniques are instrumental in revealing important relationships among multiple elements that are positively correlated with the main mineralization, ultimately aiming to identify geochemical anomalies connected to the mineral deposit model sought.

Improved multivariate statistical methods, such as the SFA [6], can be applied to discern paragenesis and key elements associated with mineral deposits [69]. SFA, an extended version of factor analysis, effectively differentiates between non-indicative (noisy) elements and significant ones pertinent to mineralization by considering the conceptual model of the deposit type being sought and employing two essential phases [18, 70]. In this research, the concentrations of 10 geochemical elements were analyzed using SFA within the framework of hydrothermal copper deposits. The results of the implementation of this method are tabulated in Table 3. According to a threshold of 0.5, Ag was excluded from the analysis, resulting in the identification of two significant factors associated with mineralization. All the elements in two factors demonstrate strong participation and have the condition of a clean factor, making them ideal for investigating hydrothermal copper mineralization. The results of the SFA imply that the association of elements in factor 1 (Zn, Pb, As, Sb, Mo, and Sn) and factor 2 (Cu, Hg, and Au) may be linked to vein-type mineralization and porphyry deposits (and possibly IOCG), respectively. Consequently, the outcomes of the SFA can guide the selection of critical elements, such

as Cu, Au, Hg, Mo, Pb, Zn, Sn, As, and Sb. By reducing the influence of non-indicator elements and geochemical noise, the geochemical layers linked to these selected elements can serve as an improved input geochemical matrix for the CAE algorithm.

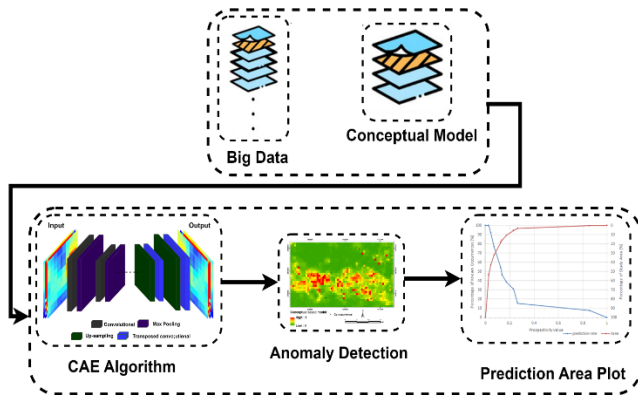


Figure 4. Workflow of this study to generate geochemical maps related to mineralization.

Table 3. The implementation of the SFA to select paragenesis elements.

SFA					
Element	First step		Element	Second Step	
	F1	F2		F1	F2
Pb	0.756	0.308	Pb	0.767	0.270
Ag	0.305	0.439	Zn	0.760	0.306
Zn	0.749	0.323	Cu	0.162	0.772
Cu	0.141	0.744	As	0.774	-0.027
As	0.775	-0.014	Sb	0.883	0.160
Sb	0.878	0.184	Hg	0.053	0.627
Hg	0.033	0.621	Au	0.195	0.735
Mo	0.774	0.196	Mo	0.779	0.197
Au	0.172	0.731	Sn	0.691	0.090
Sn	0.689	0.112	Var.	41.051	19.654
Var.	37.201	19.498	Cum.var	41.051	60.709
Cum.var	37.201	56.699	KMO	0.796	

5.2. Full dataset

Several complex geological processes and mechanisms, including structural factors, hydrothermal processes, and fluid movements, occurring over various spatial and temporal scales, influence the formation of mineralization. This leads to complex and nonlinear geochemical patterns in stream sediment data. Therefore, it is important to provide effective concepts and approaches for analyzing stream sediment geochemical data and guiding the geochemical exploration at the regional scale. In this regard, the big data analysis [31, 50, 71] is a key appropriate concept for detecting hidden and nonlinear patterns, and enhancing the accuracy of geochemical exploration. The analysis of large datasets presents substantial opportunities and potential in the domain of processing stream sediment geochemical data to improve the precision and effectiveness of regional-scale geochemical exploration [31, 71]. In contrast to traditional frameworks, the big data analysis approach focuses on the use of all geochemical elements to comprehensively reveal positive and negative geochemical anomalies and their relationship with known mineralization [71]. In addition, the big data analytics approach helps geoscientists identify hidden and nonlinear relationships between some elements that cannot be detected using classic methods. In this study, a big dataset was created in addition to a conceptual model-driven dataset (partial data), using the principles of full dataset in order to detect multi-element geochemical patterns associated with mineralization through the application of CAE (Fig. 5).

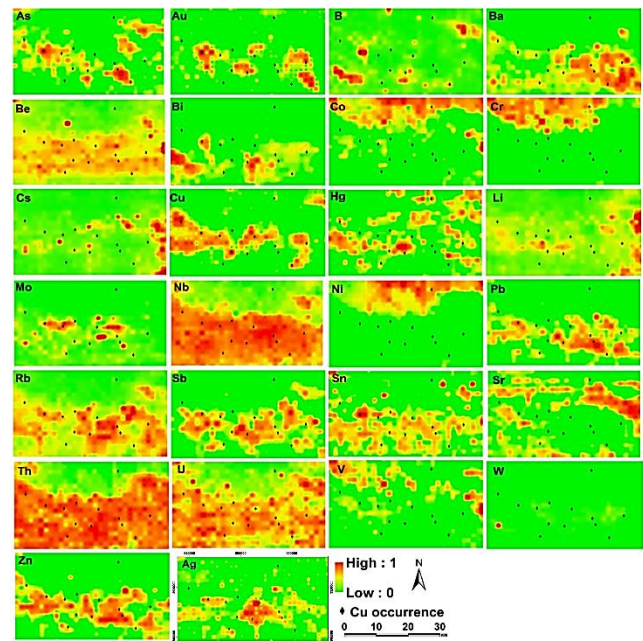


Figure 5. The distribution map of all geochemical elements in the Feizabad region. Note that the geographical coordinates were taken for the Ag map and the other layers have the same geographical coordinates.

6. Geochemical prospectivity models

This research aimed to generate two separate sets of stream sediment data to detect complex geochemical anomalies. The first dataset focused on nine specific elements (Au, Cu, Mo, As, Sb, Zn, Pb, Hg, and Sn), chosen according to the sought deposit type. In contrast, the second dataset employed a big data analytical approach, encompassing a total of 26 elements. The CAE algorithm was subsequently utilized on both datasets to identify geochemical trends that could signify the presence of significant mineralization. The CAE algorithm, recognized for its effectiveness in unsupervised anomaly detection with a geospatial emphasis [37, 48, 52, 72, 73], proved capable of identifying geochemical anomalies associated with mineralization. Consequently, the CAE algorithm facilitated the development of geochemical prospectivity models for hydrothermal copper in the northeastern region of Iran (see Figs. 6a and 6b).

The results demonstrate the effectiveness of the CAE algorithm in identifying multivariate geochemical anomalies associated with hydrothermal mineralization. Furthermore, a comparative analysis of the geochemical prospectivity models (Figs. 6a and 6b) and the simplified geological map of Feizabad at a 1:100,000 scale (Fig. 1b) reveals a strong spatial correlation between the identified anomaly regions and known mineral occurrences in both models, which are distributed across andesite, tuff, and Eocene-Oligocene intrusive rocks. These geological formations exhibit spatial and temporal relationships with copper deposits, serving as the predominant hosts for the majority of these deposits. Notably, the extent of the anomalous zones identified through the geochemical prospectivity model based on the conceptual model is smaller than that identified using the big data analytic approach.

To quantitatively assess two models, the locations of 13 known mineral deposits/occurrences in the Feizabad district were utilized as ground truth samples to draw the data-driven prediction-area "P-A" plot [74-76]. The intersection point within this plot serves as a strong criterion for evaluating the efficacy of geochemical models in predicting known mineral deposits. According to the intersection points illustrated in Figs. 7a and 7b, the prediction rates for the multi-element geochemical map derived from the conceptual model and the big data approach were 72% and 63%, respectively.

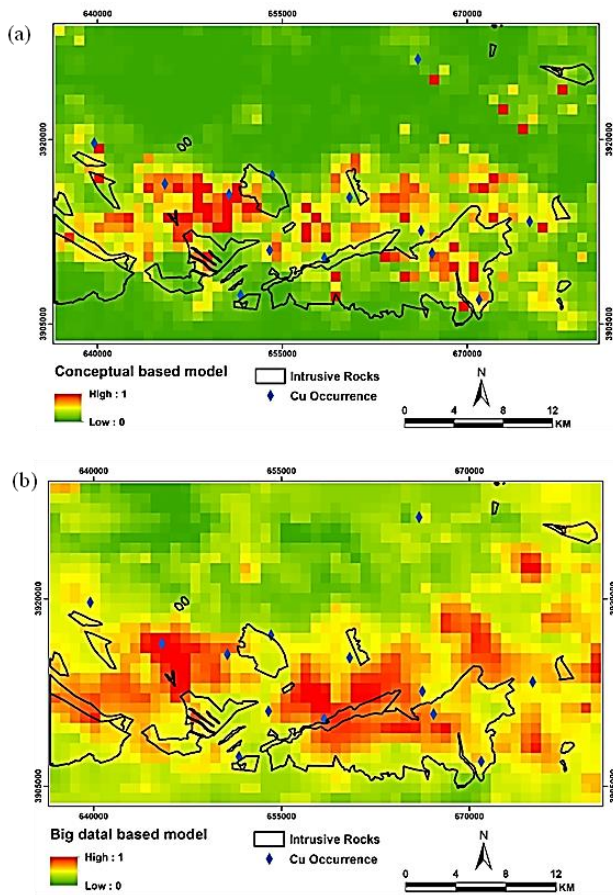


Figure 6. Two geochemical prospectivity models generated by a) The conceptual model and b) The big data approach.

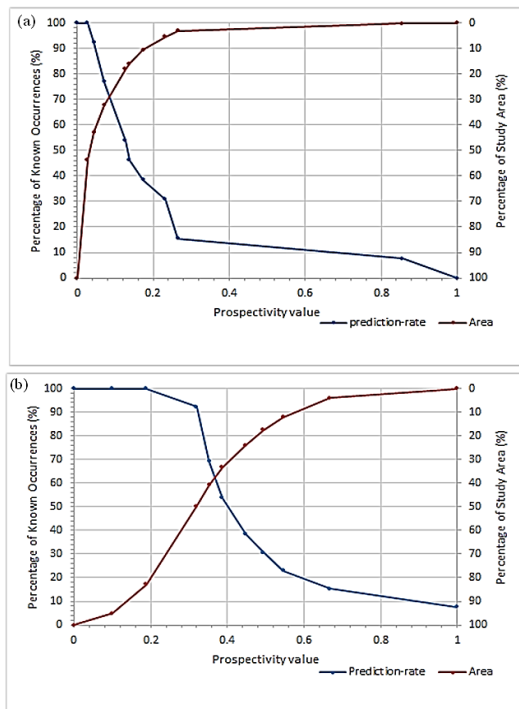


Figure 7. The prediction-area plot for two geochemical prospectivity models a) The conceptual model and b) The big data approach.

The C-A fractal method is commonly employed for classifying prospectivity models or geochemical maps and determining optimal thresholds to discretize these models [74, 77, 78]. Thresholds derived from the C-A fractal models (Figures 8b and 8d) were applied to classify the prospectivity models (Figures 8a and 8c). These thresholds divide the prospectivity values into meaningful categories, enabling a better interpretation of potential mineral zones. The fractal approach allows for a clear distinction between high (red and orange), moderate (yellow), and low (green and dark green) potential zones, contributing to more accurate exploration targeting.

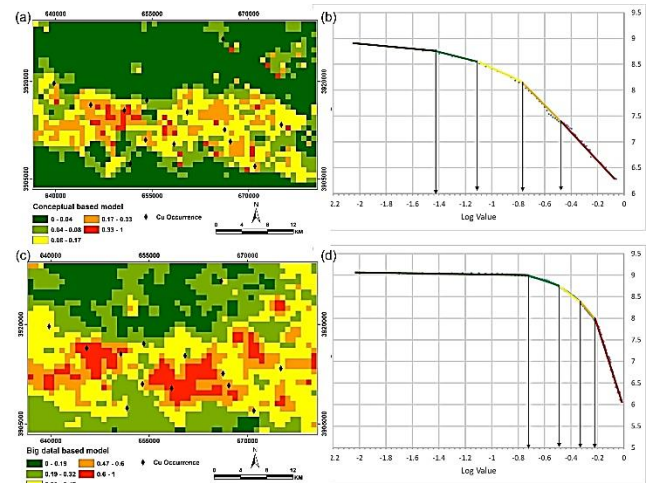


Figure 8. The fractal analysis for hydrothermal copper potential mapping: (a) the reclassified conceptual map through fractal analysis, (b) the log-log plot of C-A fractal model for the conceptual model, (c) the reclassified big data map through the fractal analysis, and (d) the log-log plot of the C-A fractal model for the big data model.

7. Discussion

Convolutional Autoencoder (CAE) is a form of unsupervised neural network employed in anomaly detection tasks within nonlinear and intricate geochemical datasets, without reliance on ground truth samples. This spatial-based algorithm functions independently of labeled datasets containing positive (deposit) and negative (non-deposit) points, thereby surpassing the constraints of supervised geochemical anomaly detection methods. Consequently, it is capable of accurately detecting patterns and anomalies associated with mineralization. Additionally, the CAE takes into account the spatial structure present in geochemical datasets, such as zoning patterns [79], leading to improved recognition of multivariate geochemical anomalies and intricate patterns.

There are several concepts and approaches in the context of generating geochemical datasets. Among these, the main approaches include: (1) utilizing the big data analytics approach [71] and (2) the conceptual model of the deposit type sought [37]. The first strategy is a novel approach to recognizing geochemical anomalies related to mineralization through considering the analysis of full geochemical datasets. Considering the positive and negative geochemical anomalies may help mitigate uncertainty in geochemical exploration. In this regard, Zuo and Xiong (2018) [71] utilized the big data analytics concept with a geochemical dataset of 39 variables to generate an anomaly map through the deep AE network in the Fujian Province, China. In addition, they produced another anomaly map using five selected elements related to mineralization. The analysis of the receiver operating characteristic (ROC) diagram and the area under curve (AUC) values indicated that the model produced from all elements outperforms the geochemical model based on only five selected elements. However, this approach has several limitations. Unsupervised models may tend to extract some anomalies that are not related to mineralization [11]. As a

result, this approach may not always be a golden way to detect geochemical anomalies with unsupervised methods [11]. Among all elements, certain ones are strong footprints of mineralization and can guide the exploration, while the remaining ones may reflect other geological events [38]. Consequently, adopting the conceptual model approach with improved multivariate analysis techniques (e.g., SFA) could be more effective for selecting key elements with strong footprints of the mineralization sought.

In this research, two geochemical models were generated using a big data analytics strategy and a conceptual model approach. Analysis of the obtained results revealed that both models successfully identified anomalous zones. The geochemical model derived from all elements shows a strong spatial correlation with some known mineral deposits/occurrences and can effectively guide exploration geologists in greenfield regions with limited exploration data (Fig. 6b). However, the prediction rate obtained from the prediction-area plot of the geochemical model obtained using nine elements related to hydrothermal mineralization was larger than the prediction rate of the geochemical model obtained using all elements (Figs. 7a and 7b). This demonstrates that the model based on the conceptual framework outperforms the other model in the Feizabad region. Consequently, the combination of SFA with a conceptual model emerges as an effective approach for identifying key factors and producing geochemical maps in brownfield areas. Geochemical maps play a crucial role as supportive layers in the Mineral Potential Mapping (MPM), improving the accuracy of the prospectivity models generated. Consequently, the creation of these maps necessitates the application of robust methodologies and principles. It is generally recommended to employ both methodologies in different geological setting and then choose the model that aligns best with the evaluation criteria.

8. Conclusion

This research utilized the CAE as an unsupervised anomaly detection algorithm to examine two sets of stream sediment data in order to improve the detection of geochemical anomalies and patterns associated with hydrothermal mineralization in the Feizabad region. The key findings of this investigation are outlined as follows:

- 1-Stream sediment samples are crucial for regional-scale geochemical exploration, providing key insights and footprints into the migration patterns of elements from alteration and mineralized zones. Hence, the geochemical indicators related to these samples are important in regional-scale mineral exploration targeting.
- 2-The conceptual model approach and big data analytic strategy are two superior techniques to generate stream sediment geochemical datasets. Employing these strategies in conjunction with robust mathematical and analytical methods enables the efficient identification of multi-element geochemical anomalies associated with mineral deposits.
- 3-The CAE serves as a robust unsupervised algorithm for spatial-based anomaly detection, capable of identifying intricate and nonlinear patterns related to mineralization within stream sediment geochemical datasets. This method can be applied in greenfield and brownfield areas to identify multi-element geochemical signatures.

Acknowledgements

The authors would like to thank the Geological Survey of Iran (GSI) for providing the geochemical data used in this paper.

References

- [1] Ayari, J., M. Barbieri, A. Barhoumi, W. Belkhiria, A. Braham, F. Dhaha, and A. Charef. (2022). A regional-scale geochemical survey of stream sediment samples in Nappe zone, northern Tunisia: Implications for mineral exploration. *Journal of Geochemical Exploration*, 235,106956.
- [2] Saremi, M., S. Yousefi, and M. Yousefi. (2024). Combination of geochemical and structural data to determine the exploration target of copper hydrothermal deposits in the Feizabad district. *Journal of Mining and Environment*, 15(3), 1089-1101.
- [3] Carranza, E.J.M. and M. Hale. (1997). A catchment basin approach to the analysis of reconnaissance geochemical-geological data from Albay Province, Philippines. *Journal of Geochemical Exploration*, 60(2),157-171.
- [4] Yousefi, M., E.J.M. Carranza, and A. Kamkar-Rouhani. (2013). Weighted drainage catchment basin mapping of geochemical anomalies using stream sediment data for mineral potential modeling. *Journal of Geochemical Exploration*, 128,88-96.
- [5] Ranasinghe, P., G. Fernando, C. Dissanayake, and M. Rupasinghe. (2008). Stream sediment geochemistry of the Upper Mahaweli River Basin of Sri Lanka—Geological and environmental significance. *Journal of Geochemical Exploration*, 99(1-3),1-28.
- [6] Yousefi, M., A. Kamkar-Rouhani, and E.J.M. Carranza. (2014). Application of staged factor analysis and logistic function to create a fuzzy stream sediment geochemical evidence layer for mineral prospectivity mapping. *Geochemistry: Exploration, Environment, Analysis*, 14(1),45-58.
- [7] Yousefi, M., A. Kamkar-Rouhani, and E.J.M. Carranza. (2012). Geochemical mineralization probability index (GMPI): a new approach to generate enhanced stream sediment geochemical evidential map for increasing probability of success in mineral potential mapping. *Journal of Geochemical Exploration*, 115,24-35.
- [8] Daviran, M., R. Ghezelbash, and A. Maghsoudi. (2023). GWOKM: A novel hybrid optimization algorithm for geochemical anomaly detection based on Grey wolf optimizer and K-means clustering. *Geochemistry*,126036.
- [9] Chen, Z., Y. Xiong, B. Yin, S. Sun, and R. Zuo. (2023). Recognizing geochemical patterns related to mineralization using a self-organizing map. *Applied Geochemistry*, 151,105621.
- [10] Zuo, R., J. Wang, Y. Xiong, and Z. Wang. (2021). The processing methods of geochemical exploration data: Past, present, and future. *Applied Geochemistry*, 132,105072.
- [11] Wang, J., Y. Zhou, and F. Xiao. (2020). Identification of multi-element geochemical anomalies using unsupervised machine learning algorithms: A case study from Ag–Pb–Zn deposits in north-western Zhejiang, China. *Applied Geochemistry*, 120,104679.
- [12] Chen, Y., L. Lu, and X. Li. (2014). Application of continuous restricted Boltzmann machine to identify multivariate geochemical anomaly. *Journal of Geochemical Exploration*, 140,56-63.
- [13] Zuo, R. and J. Wang. (2016). Fractal/multifractal modeling of geochemical data: A review. *Journal of Geochemical Exploration*, 164,33-41.
- [14] Grunsky, E. and P.d. Caritat. (2020). State-of-the-art analysis of geochemical data for mineral exploration. *Geochemistry: Exploration, Environment, Analysis*, 20(2),217-232.
- [15] Hawkes, H. and J. Webb. (1963). *Geochemistry in mineral exploration*. Soil Science, 95(4),283.
- [16] Reimann, C., H. Kürzl, and F. Wurzer, Applications of exploratory data analysis to regional geochemical mapping, in *Geochemistry and Health* (1988). 2017, CRC Press. p. 21-28.
- [17] Zuo, R. (2011). Identifying geochemical anomalies associated with Cu and Pb–Zn skarn mineralization using principal component analysis and spectrum–area fractal modeling in the Gangdese Belt, Tibet (China). *Journal of Geochemical Exploration*, 111(1-2),13-22.

- [18] Saremi, M., M. Yousefi, and S. Yousefi. (2023). Separation of geochemical anomalies related to hydrothermal copper mineralization using staged factor analysis in Feyzabad geological map. *Journal of Analytical and Numerical Methods in Mining Engineering*.
- [19] Hoseinzade, Z. and A.R. Mokhtari. (2017). A comparison study on detection of key geochemical variables and factors through three different types of factor analysis. *Journal of African Earth Sciences*, 134,557-563.
- [20] Liu, Q., G. Wu, Z. Liu, X. Mao, J. Yang, and M. Deng. (2024). Local phase-constrained convolutional autoencoder network for identifying multivariate geochemical anomalies. *Computers & Geosciences*,105679.
- [21] Esmaeiloghli, S., S.H. Tabatabaei, E.J.M. Carranza, S. Hosseini, and Y. Deville. (2021). Spatially-weighted factor analysis for extraction of source-oriented mineralization feature in 3D coordinates of surface geochemical signal. *Natural Resources Research*, 30(6),3925-3953.
- [22] Cheng, Q., F. Agterberg, and S. Ballantyne. (1994). The separation of geochemical anomalies from background by fractal methods. *Journal of Geochemical exploration*, 51(2),109-130.
- [23] Afzal, P., M. Mirzaei, M. Yousefi, A. Adib, M. Khalajmasoumi, A.Z. Zarifi, P. Foster, and A.B. Yasrebi. (2016). Delineation of geochemical anomalies based on stream sediment data utilizing fractal modeling and staged factor analysis. *Journal of African Earth Sciences*, 119,139-149.
- [24] Meigooni, M.S., P. Afzal, M. Gholinejad, A.B. Yasrebi, and B. Sadeghi. (2014). Delineation of geochemical anomalies using factor analysis and multifractal modeling based on stream sediments data in Sarajeh 1: 100,000 sheet, Central Iran. *Arabian Journal of Geosciences*, 7,5333-5343.
- [25] Ahmadi, F., H. Aghajani, and M. Abedi. (2021). Geochemical potential mapping of iron-oxide targets by Prediction-Area plot and Concentration-Number fractal model in Esfordi, Iran. *International Journal of Mining and Geo-Engineering*, 55(2),171-181.
- [26] Shamseddin Meigooni, M., M. Lotfi, P. Afzal, N. Nezafati, and M.K. Razi. (2021). Application of multivariate geostatistical simulation and fractal analysis for detection of rare-earth element geochemical anomalies in the Esfordi phosphate mine, Central Iran. *Geochemistry: Exploration, Environment, Analysis*, 21(2),geochem2020-035.
- [27] Zuo, R., Y. Xiong, J. Wang, and E.J.M. Carranza. (2019). Deep learning and its application in geochemical mapping. *Earth-science reviews*, 192,1-14.
- [28] Hajhosseinlou, M., A. Maghsoudi, and R. Ghezelbash. (2024). A comprehensive evaluation of OPTICS, GMM and K-means clustering methodologies for geochemical anomaly detection connected with sample catchment basins. *Geochemistry*,126094.
- [29] He, M.-Y., J.-B. Dong, Z. Jin, C.-Y. Liu, J. Xiao, F. Zhang, H. Sun, Z.-Q. Zhao, L.-F. Gou, and W.-G. Liu. (2021). Pedogenic processes in loess-paleosol sediments: Clues from Li isotopes of leachate in Luochuan loess. *Geochimica et Cosmochimica Acta*, 299,151-162.
- [30] Afzal, P., S. Farhadi, M. Boveiri Konari, M. Shamseddin Meigooni, and L. Daneshvar Saein. (2022). Geochemical anomaly detection in the Irankuh District using Hybrid Machine learning technique and fractal modeling. *Geopersia*, 12(1),191-199.
- [31] Xiong, Y. and R. Zuo. (2020). Recognizing multivariate geochemical anomalies for mineral exploration by combining deep learning and one-class support vector machine. *Computers & geosciences*, 140,104484.
- [32] Esmaeiloghli, S., S.H. Tabatabaei, and E.J.M. Carranza. (2023). Infomax-based deep autoencoder network for recognition of multi-element geochemical anomalies linked to mineralization. *Computers & Geosciences*, 175,105341.
- [33] Farhadi, S., S. Tatullo, M.B. Konari, and P. Afzal. (2024). Evaluating StackingC and ensemble models for enhanced lithological classification in geological mapping. *Journal of Geochemical Exploration*, 260,107441.
- [34] Li, S., J. Chen, and J. Xiang. (2020). Applications of deep convolutional neural networks in prospecting prediction based on two-dimensional geological big data. *Neural computing and applications*, 32,2037-2053.
- [35] Mirzabozorg, S.A.A.S., M. Abedi, and M. Yousefi. (2024). Enhancing training performance of convolutional neural network algorithm through an autoencoder-based unsupervised labeling framework for mineral exploration targeting. *Geochemistry*,126197.
- [36] Zhao, J., S. Chen, and R. Zuo. (2016). Identifying geochemical anomalies associated with Au–Cu mineralization using multifractal and artificial neural network models in the Ningqiang district, Shaanxi, China. *Journal of Geochemical Exploration*, 164,54-64.
- [37] Guan, Q., S. Ren, L. Chen, B. Feng, and Y. Yao. (2021). A spatial-compositional feature fusion convolutional autoencoder for multivariate geochemical anomaly recognition. *Computers & Geosciences*, 156,104890.
- [38] Mirzabozorg, S.A.A.S. and M. Abedi. (2023). Recognition of mineralization-related anomaly patterns through an autoencoder neural network for mineral exploration targeting. *Applied Geochemistry*,105807.
- [39] Chen, Y. and W. Wu. (2017). Application of one-class support vector machine to quickly identify multivariate anomalies from geochemical exploration data. *Geochemistry: Exploration, Environment, Analysis*, 17(3),231-238.
- [40] Chen, Y., S. Wang, Q. Zhao, and G. Sun. (2021). Detection of multivariate geochemical anomalies using the bat-optimized isolation forest and bat-optimized elliptic envelope models. *Journal of Earth Science*, 32(2),415-426.
- [41] Shahrestani, S. and E.J.M. Carranza. (2024). Effectiveness of LOF, iForest, and OCSVM in detecting anomalies in stream sediment geochemical data. *Geochemistry: Exploration, Environment, Analysis*, geochem2024-009.
- [42] Bigdeli, A., A. Maghsoudi, and R. Ghezelbash. (2022). Application of self-organizing map (SOM) and K-means clustering algorithms for portraying geochemical anomaly patterns in Moalleman district, NE Iran. *Journal of Geochemical Exploration*, 233,106923.
- [43] Rezapour, M.J., M. Abedi, A. Bahroudi, and H. Rahimi. (2020). A clustering approach for mineral potential mapping: A deposit-scale porphyry copper exploration targeting. *Geopersia*, 10(1),149-163.
- [44] Agha Seyyed Mirzabozorg, S., M. Abedi, and F. Ahmadi. (2023). Clustering of Areas Prone to Iron Mineralization in Esfordi Range based on a Hybrid Method of Knowledge-and Data-Driven Approaches. *Journal of Mineral Resources Engineering*, 8(4),1-26.
- [45] Aryafar, A., H. Moeini, and V. Khosravi. (2020). CRFA-CRBM: a hybrid technique for anomaly recognition in regional geochemical exploration; case study: Dehsalm area, east of Iran. *International Journal of Mining and Geo-Engineering*, 54(1),33-38.
- [46] Aryafar, A. and H. Moeini. (2017). Application of continuous restricted Boltzmann machine to detect multivariate anomalies from stream sediment geochemical data, Korit, East of Iran. *Journal of Mining and Environment*, 8(4),673-682.

- [47] Xiong, Y. and R. Zuo. (2016). Recognition of geochemical anomalies using a deep autoencoder network. *Computers & Geosciences*, 86,75-82.
- [48] Xiong, Y. and R. Zuo. (2021). Robust feature extraction for geochemical anomaly recognition using a stacked convolutional denoising autoencoder. *Mathematical Geosciences*,1-22.
- [49] Saremi, M., Z. Hoseinzade, S.A.A.S. Mirzabozorg, A.B. Pour, B. Zoheir, and A. Almasi. (2024). Integrated remote sensing and geochemical studies for enhanced prospectivity mapping of porphyry copper deposits: a case study from the Pariz district, Urmia-Dokhtar metallogenic belt, southern Iran. *Remote Sensing Applications: Society and Environment*,101343.
- [50] Xiong, Y., R. Zuo, and E.J.M. Carranza. (2018). Mapping mineral prospectivity through big data analytics and a deep learning algorithm. *Ore Geology Reviews*, 102,811-817.
- [51] Yu, X., P. Yu, K. Wang, W. Cao, and Y. Zhou. (2024). Data-Driven Mineral Prospectivity Mapping Based on Known Deposits Using Association Rules. *Natural Resources Research*,1-24.
- [52] Chen, L., Q. Guan, B. Feng, H. Yue, J. Wang, and F. Zhang. (2019). A multi-convolutional autoencoder approach to multivariate geochemical anomaly recognition. *Minerals*, 9(5),270.
- [53] Maghsoudi, A., M. Rahmani, and B. Rashidi, Gold deposits and indications of Iran. 2005.
- [54] Behroozi, A. (1987). Geological map of Iran 1: 100,000 series, Feizabad. Geological Survey of Iran, Tehran.
- [55] Karimpour, M.H., A.M. Shafaroudi, A.M. Bajestani, R.K. Schader, C.R. Stern, L. Farmer, and M. Sadeghi. (2017). Geochemistry, geochronology, isotope and fluid inclusion studies of the Kuh-e-Zar deposit, Khaf-Kashmar-Bardaskan magmatic belt, NE Iran: Evidence of gold-rich iron oxide-copper-gold deposit. *Journal of Geochemical Exploration*, 183,58-78.
- [56] Taghadosi, H. and A. Malekzadeh Shafaroudi. (2018). Evidences of probable porphyry Cu-Au mineralization in Namegh area, Northeast of Kashmir: geology, Alteration, mineralization, geochemistry, and fluids inclusion studies. *Scientific Quarterly Journal of Geosciences*, 27(108),105-114.
- [57] Yousefi, M. and V. Nykänen. (2016). Data-driven logistic-based weighting of geochemical and geological evidence layers in mineral prospectivity mapping. *Journal of Geochemical Exploration*, 164,94-106.
- [58] Zhang, Y. A better autoencoder for image: Convolutional autoencoder. in *ICONIP17-DCEC*. 2018.
- [59] Zhao, B., D. Zhang, P. Tang, X. Luo, H. Wan, and L. An. (2023). Recognition of multivariate geochemical anomalies using a geologically-constrained variational autoencoder network with spectrum separable module—A case study in Shangluo District, China. *Applied Geochemistry*, 156,105765.
- [60] Zeiler, M.D. and R. Fergus. Visualizing and understanding convolutional networks. in *Computer Vision—ECCV 2014: 13th European Conference, Zurich, Switzerland, September 6-12, 2014, Proceedings, Part I* 13. 2014. Springer.
- [61] Yousefi, M. (2017). Recognition of an enhanced multi-element geochemical signature of porphyry copper deposits for vectoring into mineralized zones and delimiting exploration targets in Jiroft area, SE Iran. *Ore Geology Reviews*, 83,200-214.
- [62] Yousefi, M., A. Kamkar-Rouhani, and M. Alipoor. (2014). Increasing the Exploration Success and Intensify of Stream Sediment Geochemical Halos Using Recognizing and Omitting the Non-Predictive Factors, Case Studies: Fluorite and Copper Mineralization. *Scientific Quarterly Journal of Geosciences*, 24(93),85-92.
- [63] Parsa, M., A. Maghsoudi, M. Yousefi, and M. Sadeghi. (2016). Recognition of significant multi-element geochemical signatures of porphyry Cu deposits in Noghdoz area, NW Iran. *Journal of Geochemical Exploration*, 165,111-124.
- [64] Shahrestani, S., D.R. Cohen, and A.R. Mokhtari. (2024). A comparison of PCA and ICA in geochemical pattern recognition of soil data: The case of Cyprus. *Journal of Geochemical Exploration*, 264,107539.
- [65] Hajihosseini, M., A. Maghsoudi, and R. Ghezelbash. (2024). Regularization in machine learning models for MVT Pb-Zn prospectivity mapping: applying lasso and elastic-net algorithms. *Earth Science Informatics*,1-15.
- [66] Pirdadeh Beyranvand, D., M.A. Arian, T. Farhadinejad, and A. Ashja Ardalan. (2021). Identification of Geochemical Distribution of REEs Using Factor Analysis and Concentration-Number (CN) Fractal Modeling in Granitoids, South of Varcheh 1: 100000 Sheet, Central Iran. *Iranian Journal of Earth Sciences*, 13(4),288-289.
- [67] Saadati, H., P. Afzal, H. Torshizian, and A. Solgi. (2020). Geochemical exploration for lithium in NE Iran using the geochemical mapping prospectivity index, staged factor analysis, and a fractal model. *Geochemistry: Exploration, Environment, Analysis*, 20(4),461-472.
- [68] Saremi, M., A. Maghsoudi, Z. Hoseinzade, and A.R. Mokhtari. (2024). Data-driven AHP: a novel method for porphyry copper prospectivity mapping in the Varzaghan District, NW Iran. *Earth Science Informatics*,1-16.
- [69] Koohzadi, F., P. Afzal, D. Jahani, and M. Pourkermani. (2021). Geochemical exploration for Li in regional scale utilizing Staged Factor Analysis (SFA) and Spectrum-Area (SA) fractal model in north central Iran. *Iranian Journal of Earth Sciences*, 13(4),299-307.
- [70] Saremi, M., A. Maghsoudi, R. Ghezelbash, M. Yousefi, and A. Hezarkhani. (2024). Targeting of porphyry copper mineralization using a continuous-based logistic function approach in the Varzaghan district, north of Urumieh-Dokhtar magmatic arc. *Journal of Mining and Environment*.
- [71] Zuo, R. and Y. Xiong. (2018). Big data analytics of identifying geochemical anomalies supported by machine learning methods. *Natural Resources Research*, 27,5-13.
- [72] Zhang, C., R. Zuo, and Y. Xiong. (2021). Detection of the multivariate geochemical anomalies associated with mineralization using a deep convolutional neural network and a pixel-pair feature method. *Applied Geochemistry*, 130,104994.
- [73] Zhang, S., E.J.M. Carranza, H. Wei, K. Xiao, F. Yang, J. Xiang, S. Zhang, and Y. Xu. (2021). Data-driven mineral prospectivity mapping by joint application of unsupervised convolutional auto-encoder network and supervised convolutional neural network. *Natural Resources Research*, 30,1011-1031.
- [74] Yousefi, M. and E.J.M. Carranza. (2015). Prediction-area (P-A) plot and C-A fractal analysis to classify and evaluate evidential maps for mineral prospectivity modeling. *Computers & Geosciences*, 79,69-81.
- [75] Roshanravan, B., H. Aghajani, M. Yousefi, and O. Kreuzer. (2019). An improved prediction-area plot for prospectivity analysis of mineral deposits. *Natural Resources Research*, 28,1089-1105.
- [76] Hoseinzade, Z., A. Zavarei, and K. Shirani. (2021). Application of prediction-area plot in the assessment of MCDM methods through VIKOR, PROMETHEE II, and permutation. *Natural Hazards*, 109,2489-2507.
- [77] Afzal, P., A. Khakzad, P. Moarefvand, N.R. Omran, B. Esfandiari, and Y.F. Alghalandis. (2010). Geochemical anomaly separation by

multifractal modeling in Kahang (Gor Gor) porphyry system, Central Iran. *Journal of Geochemical Exploration*, 104(1-2),34-46.

- [78] Afzal, P., M. Abdideh, and L. Daneshvar Saein. (2023). Separation of productivity index zones using fractal models to identify promising areas of fractured reservoir rocks. *Journal of Petroleum Exploration and Production Technology*, 13(9),1901-1910.
- [79] Li, H., X. Li, F. Yuan, S.M. Jowitt, M. Zhang, J. Zhou, T. Zhou, X. Li, C. Ge, and B. Wu. (2020). Convolutional neural network and transfer learning based mineral prospectivity modeling for geochemical exploration of Au mineralization within the Guandian–Zhangbaling area, Anhui Province, China. *Applied Geochemistry*, 122,104747.